ACTA STEREOL 1998; 17/1: 75-82
ORIGINAL SCIENTIFIC PAPER

AN OBSERVER-INDEPENDENT CYTOARCHITECTONIC MAPPING OF THE HUMAN CORTEX USING A STEREOLOGICAL APPROACH.

Axel Schleicher [1], Katrin Amunts[1], Stephan Geyer [2], Tilo Kowalski[1], Karl Zilles[12]

[1] C. & O. Vogt Institute for Brain Research, University of Düsseldorf, P.O. Box 101007, D-40001 Düsseldorf, Germany, [2] Department of Neuroanatomy, University of Düsseldorf, Düsseldorf, Germany.
e-mail: axel@hirn.uni-duesseldorf.de

Abstract

Cytoarchitectonic areas of the cerebral cortex cannot be identified in PET or fMRI images. Architectonic identification, however, is necessary if imaging data are to be interpreted as functions of anatomical entities. Functional/structural correlation requires the superimposition of cytoarchitecturally defined cortical areas with functional data in a common reference system. Up to now, most delineations of areas were based on the observer's ability to detect subtle differences in cytoarchitecture. In order to exclude observer-dependent effects on mapping, we developed a fully automated stereological approach with which to localise the borders of cortical areas.

A cortical area is characterised by a distinct laminar pattern. This pattern is represented by profile curves extending from the beginning of layer II to the white matter boundary. Histological sections were digitised using the grey level index procedure, and the profiles are constructed from these images. The shapes of neighbouring profiles are compared by calculating their distances according to feature vectors extracted from the profiles. Profiles derived from a homogeneous area can be expected to be similar in shape and hence show low distance values between each other. Maximum distances can be found between profiles which lie on opposite sides of a structural boundary. The Mahalanobis distance was found to be more sensitive than other distance measures such as the Euclidean distance and to yield a defined spatial resolution.

As an example, cell-stained sections of the human occipital cortex were analysed. The method not only verified boundaries which had been defined by visual inspection, it also revealed new ones which had not been detected visually.

Key Words: Brain mapping – Cerebral cortex – Cytoarchitecture – Grey level index – Density profiles – Multivariate statistics

This work was supported by grants of the Deutsche Forschungsgemeinschaft (SFB 194/A6), of the EU-BioMed2 Program and of the EU-BioTech Program.

Introduction

The mapping of the cerebral cortex has been a challenge for many neurobiologists. Brodmann's map (1909) of the human brain subdivides the neocortex into numerous, numbered areas. It is an anatomical map. i.e., the localisation of boundaries is based on microstructural differences between areas. Although introduced almost a century ago, this map is still the most commonly used reference for interpreting functional activations as seen in PET or fMRI images. Additional anatomical maps have been drawn since Brodmann, but they differ in the number, localisation, and contours of areas. Such differences are due mainly to the fact that mapping is still based on the qualitative, visual interpretation of microscopical images, and subjective criteria introduce high levels of variability.

We present a new, observer-independent method for parcellating the cerebral cortex and demonstrate its application to histological sections of the occipital cortex including the primary visual cortex (Brodmann's area 17), area 18 and parts of area 19.

Material and Methods

The microstructural organisation of cortical areas is characterised by inhomogeneities in the distribution of cells which lead to laminar patterns. In sections these laminae become visible as layers lying parallel to the cortical surface (Fig. 1a). It is generally understood that functional differentiation is reflected by a specific microstructural organisation and thus by a specific laminar pattern. Distinct differences in laminar patterns can be found at the boundary between area 17 and the adjoining area 18 (marked by arrowheads in Fig. 1a). The most striking feature of this boundary is the disappearance of area 17's layer IVc (marked by asterisk), which is missing in area 18. Our method quantifies such changes and detects boundaries at locations where the patterns differ.

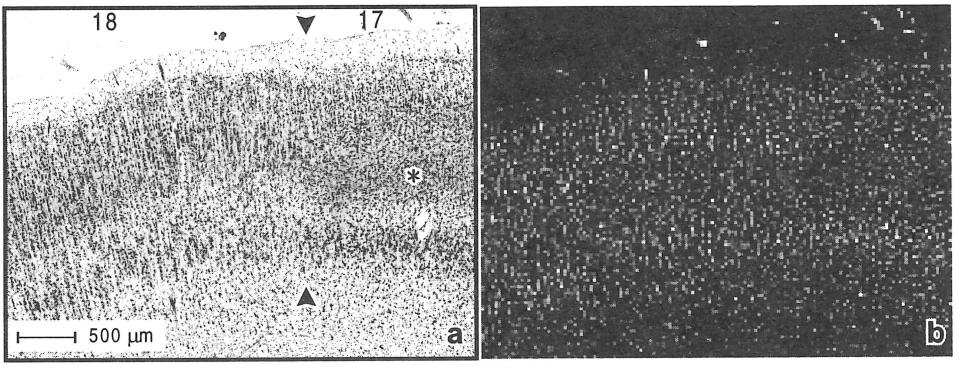

Fig 1. (a) Photomicrograph of a histological section stained for cell bodies. The boundary between area 17 and area 18 is marked by arrowheads. The asterisk marks layer IVc in area 17. **(b)**. GLI-image of (a) scanned at a spatial resolution of 25µm.

The histological section stained for cell bodies is digitised using a TV-based image analysing system. Adaptive thresholding of the microscopical image generates a binary image which is

scanned by a grid of square measuring fields (e.g. 25µm per side). The areal fraction of cellular profiles in each field is an estimate of the volume density of cell bodies and is referred to as grey level index (GLI, Schleicher and Zilles, 1989). The combined scanning of the histological section by TV frames and measuring fields results in a GLI image (Fig. 1b). The GLI values range from black (0%) to white (100%). Each pixel in the GLI image represents one measuring field in position and GLI value.

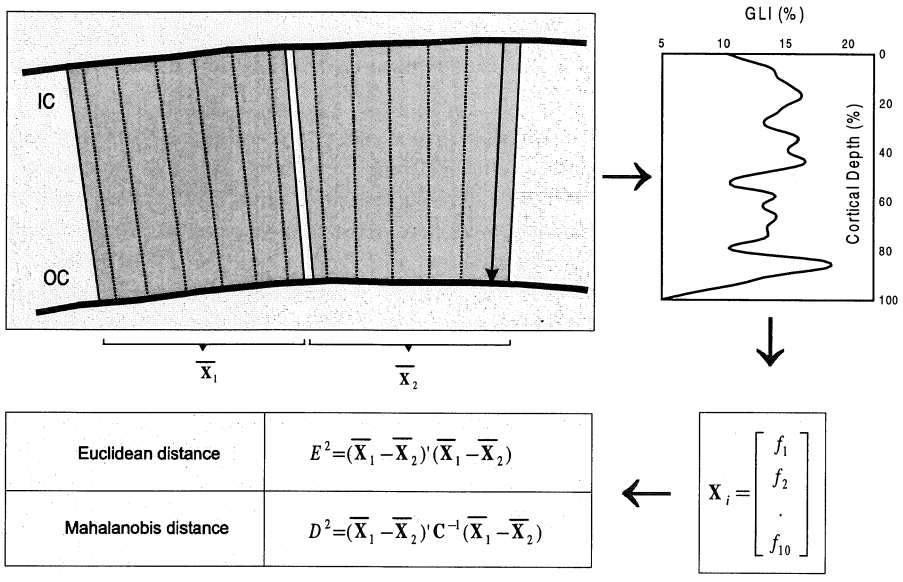

Fig 2. Calculation of the Euclidean and the Mahalanobis distance. For details see text.

The procedure for quantifying the laminar pattern and calculating the dissimilarity between two patterns is illustrated in figure 2. Two neighbouring cortical sectors are marked by shaded blocks. In each sector, a block of b (b=6 in this schematic drawing) GLI profiles is extracted along traverses extending from the top of layer II (OC) to the bottom of layer VI (IC). An example of a GLI-profile extracted from the GLI-image of area 17 illustrates the laminar pattern in this area. The cortical depth is normalised to 100%. Profile shape is quantified using a vector X_i comprising 10 features f_j ($1 \leq j \leq 10$) which are based on central moments extracted from each profile and from the absolute value of its differential quotient. Two mean vectors, $\overline{X}_1$ and $\overline{X}_2$ are calculated for the two blocks of profiles. From these two mean vectors, a measure of dissimilarity is established by calculating their Euclidean distance E^2. The Mahalanobis distance D^2 (Mahalanobis et al., 1949) is a modification of the Euclidean distance and accounts for the correlation between features because the pooled covariance matrix C was introduced. When using the Euclidean distance E^2, the block size may be narrowed down to only 1 profile, whereas the Mahalanobis distance D^2 can only be applied at 6 or more profiles per block since b is related to the number of features p by the constraint $b \geq p/2 + 1$.

The cortex is systematically scanned by calculating a sequence of distance values at predefined positions. Starting from an initial position, a distance value (Euclidean or Mahalanobis) is

calculated. The two grouped blocks are then shifted along the cortex by an increment equivalent to the space between two profiles and a new distance value is established by calculating two new mean feature vectors, $\overline{X}_1$ and $\overline{X}_2$, and a new covariance matrix C. Repeating this procedure for all positions in a region of interest results in a distance function. The abscissa indicates the position of the two blocks, the ordinate is the corresponding distance value (for an example of a distance function, see Fig. 3b). As long as the two blocks of profiles are located within a homogeneous cortical area, the laminar pattern in the two sectors will be similar and the distance values will be low and only affected by random perturbations. If the two sectors meet a cortical boundary, i.e., the two sectors lie on opposite sides of a cortical boundary, a peak distance value will mark this boundary. Thus, peak values in a distance function represent microstructural boundaries.

The characteristics of the two distance measures were examined by analysing a cortical model (Fig. 3a). A laminar pattern was composed of different grey levels and noise was added. Boundaries were predefined in layer IV, and a thinning caused by cortical folding appeared in layer II. Each of the 200 columns in the image matrix was extracted as one profile. The Euclidean distance for blocks with 8 profiles (Fig. 3b) indicated all boundaries in layer IV by peaks. An additional peak (marked by arrow at position 134) was caused exclusively by the cortical thinning in layer II, no boundary in layer IV was defined at this position. The Mahalanobis distance function (Fig. 3c) produced sharp, narrow peaks: All boundaries in layer IV were indicated, the cortical thinning at position 134 was not detected. The boundary in layer IV at position 168 (marked by arrow) was, however, detected in spite of the gradual change in the thickness of layer II at this position. The lower two plots (Figs. 3d,e) exhibit the distance functions for wider cortical sectors using blocks of 12 profiles. The distance functions are similar to those shown for blocks with 8 profiles. As a additional feature, the small cortical stretch 8 pixel wide at position 60 (Fig. 3a) was completely ignored by the Mahalanobis approach (Fig. 3e). Thus the Mahalanobis distance procedure is superior to the Euclidean one since it is not sensitive to gradual changes in the laminar pattern caused by cortical folding and it yields a defined spatial resolution.

Results

The procedure is demonstrated for the mapping of the occipital cortex. The high resolution TV scan of a histological section stained for cell bodies shown in figure 4 includes the primary visual cortex (Brodmann's area 17), area 18 and a cortical region which is part of Brodmann's area 19. OBγ is part of area 18 adjacent to area 17 and was not mentioned by Brodmann, but was microstructurally defined by von Economo and Koskinas in 1925. The transition between area 17 and OBγ can easily be recognised by visual inspection. All the other boundaries are much less obvious visually, especially the boundary between OBγ and rest of area 18 cannot be located unambiguously.

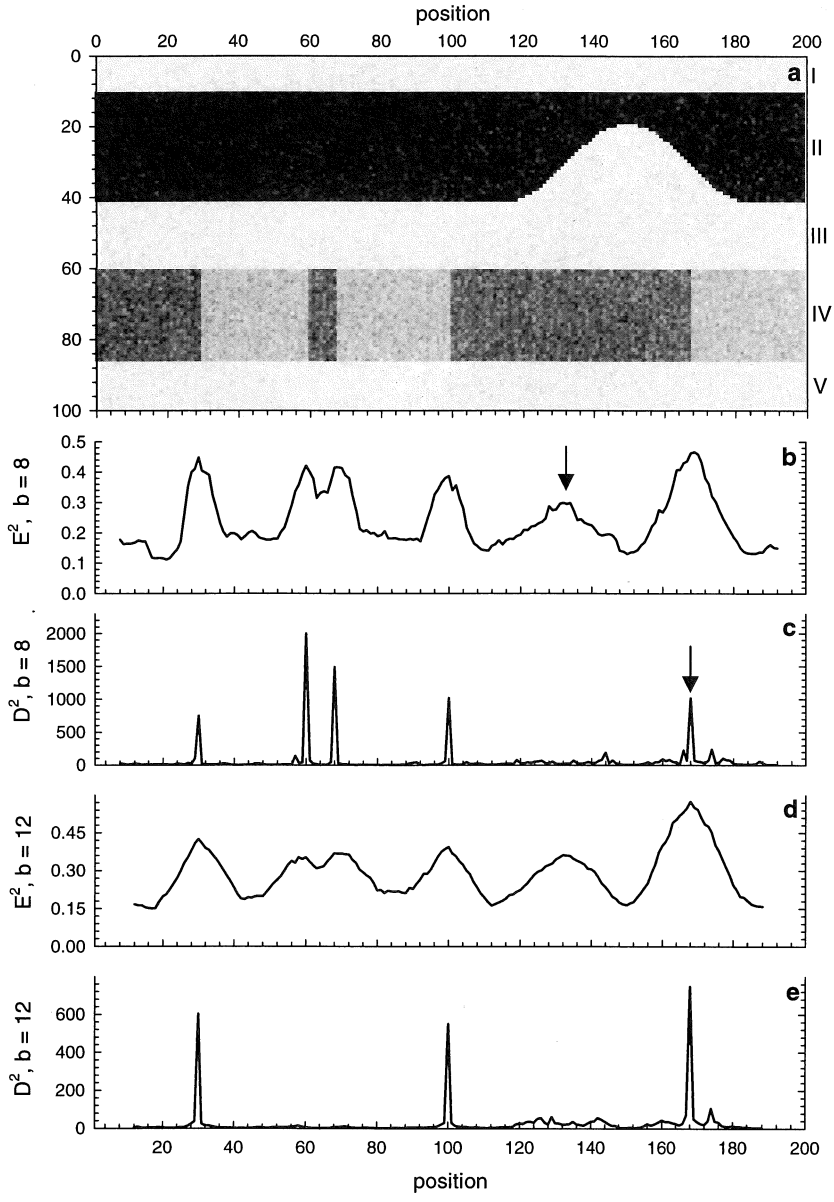

Fig. 3 (a) Model of a cortical region (100x100 pixel) with 5 layers (I-V). Sine-shaped distortion between layers II and III, cortical boundaries defined by changes in GLI values in layer IV. Each pixel column of the image was extracted as one profile. Abscissa in (a-e): position of the 200 profile. Ordinate in (a): cortical depth in %. **(b)** Euclidean distance function, b=8. Ordinate: distance E^2. **(c)** Mahalanobis distance function, b=8. Ordinate: distance D^2. **(d)** Euclidean distance function, b=12. Ordinate: distance E^2. **(e)** Mahalanobis distance function, b=12. Ordinate: distance D^2.

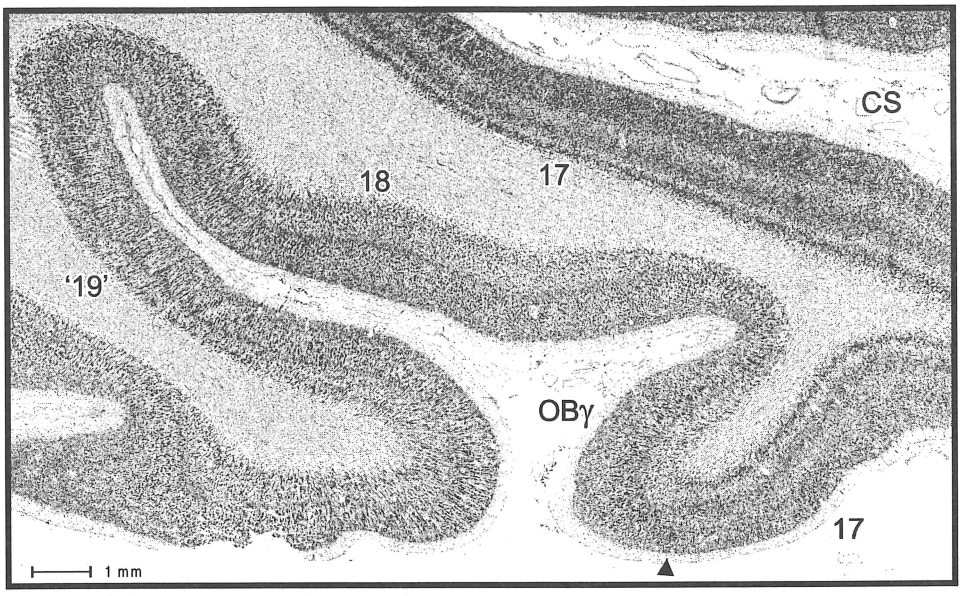

Fig. 4 Photomicrograph of silver-stained, coronal section of adult human brain showing the primary visual cortex area 17 and the adjoining areas (CS = calcarine sulcus). Arrowhead marks boundary between area 17 (right) and OBγ (left).

The scanning of these cortical areas by blocks of GLI profiles is shown in figure 5a. Numbering of the profiles begins outside area 18 and ends in area 17. The Euclidean distance function for narrow sectors comprising only 1 profile (Fig. 5b) is noisy and the large number of peaks precludes any meaningful interpretation of this pattern as a cortical parcellation. In order to improve the signal to noise ratio, wider sectors with 12 profiles each were applied. The Euclidean distance function then showed only a few broad peaks (Fig. 5c). The Mahalanobis distance function was superior to the Euclidean approach because it clearly indicated peaks which can now be assigned to distinct changes in the laminar pattern. In figure 5d position 27 is the boundary between area 19 and area 18; position 99 is the boundary between OBγ and the rest of area 18; position 113 is the boundary between OBγ and area 17. Additional peaks within area 18 also indicate changes in the laminar pattern and thus microstructural boundaries. This subparcellation also appeared in neighbouring sections. Inhomogeneity in area 18 can be detected in sections stained for myelin as well and the spacing pattern of the subparcellations in both preparations is similar.

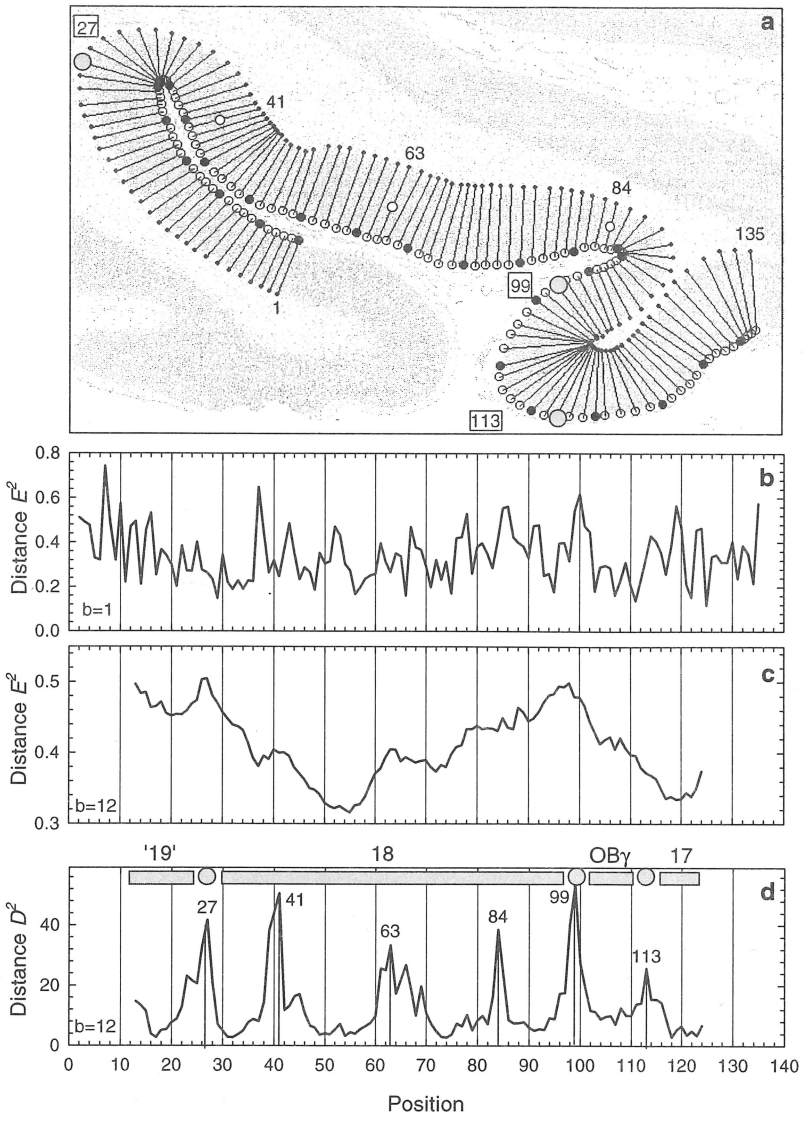

Fig. 5. (a) GLI scan of the region shown in Fig. 4, inverted and reduced in contrast, with a set of 135 superimposed traverses which cover areas 17, 18 and 19. Starting points of traverses are marked by circles, endpoints are marked by dots. Numbering of profiles begins on the left side of the GLI scan, positions 1,6,11,16... are marked by filled circles. Shaded circles mark positions 27 (border between area 18 and area 19), 99 (border between area 18 and *OBγ*) and 113 (border between *OBγ* and area 17). **(b)** Euclidean distance function for set of profiles shown in (a) calculated for each pair of neighboring individual profiles (b=1) **(c)** Euclidean distance function calculated for each pair of neighboring blocks of profiles (b=12 profiles per block). **(d)** Mahalanobis distance function for each pair of neighboring blocks of profiles (b=12 profiles per block). Main maxima are denoted by drop lines. Shaded circles label the maxima with corresponding positions marked in (a). Parcellation pattern is indicated by shaded rectangles.

Discussion

This example demonstrates that our method verifies boundaries which are obvious to visual inspection like the area 17-OBγ boundary. It is of particular value for defining boundaries which are much more difficult to detect and therefore still the subject of controversy, such as the boundary between OBγ and the rest of area 18 and the subparcellation of area 18. The localisation of these boundaries by pure visual inspection is extremely difficult or even impossible and as a consequence, parcellation patterns vary greatly. Several studies have shown the existence of microstructurally defined cortical areas which are not readily detectable in the microscope (Zilles et al., 1982). We have been able to demonstrate that the Mahalanobis approach clearly detects such boundaries. Microstructural/functional relationships are the subject of intensive investigations, and for some areas in the human cortex this relationship has already been established (e.g. Geyer et al., 1996).

Our approach is not restricted to GLI images and cytoarchitecture. We have applied it successfully to a variety of optical density images which exhibit a laminar pattern: autoradiographs, myelin staining, AChE staining, and immunohistochemical preparations.

References

Brodmann K. Vergleichende Lokalisationslehre der Großhirnrinde in ihren Prinzipien dargestellt auf Grund des Zellenbaues. Leipzig: JA Barth 1909.

von Economo K, Koskinas G. Die Cytoarchitektonik der Hirnrinde des erwachsenen Menschen, Wien: Springer 1925

Geyer S, Ledberg A, Schleicher A, Kinomura S, Schormann T, Bürgel U, Larsson J, Zilles K, Roland PE. Two different areas within the primary motor cortex of man. Nature 1996; 382: 805-807

Mahalanobis PC, Majumda DN, Rao CR. Anthropometric survey of the united provinces. A statistical study. Sankhya 1949; 9: 89-324.

Schleicher A, Zilles K. A quantitative approach to cytoarchitectonics: analysis of structural inhomogeneities in nervous tissue using an image analyser. J Microscopy 1989; 157: 367-381

Zilles K, Stephan H, Schleicher, A. Quantitative cytoarchitectonics of the cerebral cortices of several prosimian species. In: Armstrong E, Falk D, eds. Primate Brain Evolution: Methods and Concepts. New York: Plenum Press 1982: 177-201.

Presented at the 7th European Congress for Stereology, Amsterdam, April 20th to 23rd, 1998.